ARTICLES

Fluorescence Anisotropy Study of Aqueous Dispersions of Block Ionomer Complexes

Sergey V. Solomatin,[†] Tatiana K. Bronich,[†] Adi Eisenberg,[§] Victor A. Kabanov,[#] and Alexander V. Kabanov*[,†]

Department of Pharmaceutical Sciences, College of Pharmacy, 986025 Nebraska Medical Center, Omaha, Nebraska 68198-6025, Department of Chemistry, McGill University, 801 Sherbrooke Street West, Montreal, Quebec, Canada H3A 2K6, and Department of Polymer Sciences, School of Chemistry, M.V. Lomonosov Moscow State University, Leninskie Gory, Moscow V-234, 119899 Russia

Received: May 11, 2004; In Final Form: October 25, 2004

Block ionomer complexes (BIC) of "dual hydrophilic" block copolymers containing ionic and nonionic blocks and oppositely charged surfactants spontaneously form colloidal particles of ca. 80 nm in diameter stable in aqueous dispersions at every composition of the mixture. Packing and dynamics of aliphatic groups of the surfactant in BIC were examined by using the quenching-resolved fluorescence anisotropy (QRFA) method with 1,6-diphenyl-1,3,5-hexatriene (DPH) as a probe. The values of the order parameter and rotational relaxation time in the BIC were higher than those in the surfactant micelles. Incorporation of aliphatic alcohols in the BIC decreased the order parameter and increased the rotational relaxation time. The effects on the order parameter were explained by changes in the surfactant aliphatic group conformation to "fill the gaps" induced by insertion of shorter alcohol molecules. The effects on the relaxation time were attributed to a decrease in repulsion of the surfactant headgroups and expulsion of water from the BIC hydrophobic interior as evidenced by the decrease in micropolarity. The results of this study have implications for potential use of the BIC in pharmaceutics and other fields.

Introduction

Complexes of polyelectrolytes with oppositely charged surfactants have significant potential in engineering, cosmetics, detergent formulation, drug delivery, and other applications.[1] At low surfactant-to-polymer charge ratios the complexes are soluble and represent individual surfactant micelles bound to the polymer chains ("pearls on a necklace" model).[2−5] The bound micelles appear to retain the original shape although they can be marginally larger[4] or smaller[6] than the free micelles. Some decrease in the surfactant mobility in such complexes was reported, but overall, the packing of the surfactant molecules was not significantly perturbed.[7] At higher surfactant-to-polymer charge ratios the complexes usually become water insoluble and precipitate.[8,9] Under these conditions the surfactant molecules form semicrystalline lamellar arrays and display reduced mobility compared to the micelles.[7,10−14]

The block ionomer complexes (BIC) were synthesized recently by reacting "dual hydrophilic" block copolymers with ionic and nonionic blocks and oppositely charged surfactants.[15−18] Such complexes can form micelles[19] or vesicles[20] depending on the structure of the block copolymer and surfactant and they remain stable in aqueous dispersions at any charge ratio, including stoichiometric compositions.[15,17] It has been shown that BIC particles are stabilized in the dispersed state by hydrophilic nonionic chains, e.g., poly(ethylene oxide) (PEO) forming a protective corona.[21] However, little is known about the structure of the surfactant domains in such complexes. Some studies suggested that the surfactants are packed into spherical micelles, neutralized, and bridged together by the polyion chains.[22,23] Others proposed that the polyion chains are laterally absorbed onto the lamellar arrays formed by the surfactants.[15,17]

To address this we examined the dynamics and packing of aliphatic groups of the surfactant by using the quenching-resolved fluorescence anisotropy (QRFA) technique[24,25] with 1,6-diphenyl-1,3,5-hexatriene (DPH) as a probe. The method was previously used to characterize lipid membranes and other surfactant aggregates.[26−32] The present work applied this method to BIC formed by PEO-*b*-poly(sodium methacrylate) (PEO-*b*-PMA) and hexadecyltrimethylammonium bromide (HTAB). The results suggest that the packing and mobility of the surfactant aliphatic groups in BIC were significantly altered compared to those in the micelles. These parameters can be further modified by incorporating aliphatic alcohols of different lengths in the BIC. Overall, the results are useful for potential application of BIC in drug delivery and other areas.

Materials and Methods

Materials. Block ionomer PEO_{210}-*b*-PMA_{97} was synthesized as reported previously.[33] HTAB (Sigma Co., 99% pure), *N*-hexadecylpyridinium bromide (C_{16}PyBr, Aldrich Co., 98% pure), and DPH (Molecular Probes) were used without further purification. 1-Butanol (98%), 1-hexanol (99%+), 1-octanol

* Corresponding author: Fax: (402) 559-9543. E-mail: akabanov@unmc.edu.
[†] University of Nebraska Medical Center.
[§] McGill University.
[#] Moscow State University.

10.1021/jp047980k CCC: $30.25
Published on Web 02/19/2005

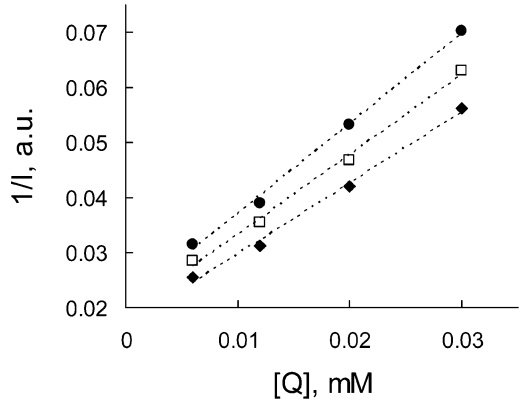

Figure 1. The effect of the $C_{16}Py^+$ concentration on the intensity of the DPH fluorescence in the BIC at 25 (solid diamonds), 30 (open squares), and 35 °C (solid circles). The dashed lines represent the least-squares fit ($R^2 > 0.99$ in each case). [Q] is the concentration of the quencher; au = arbitrary fluorescence units. $C_{PMA} = C_{HTAB} = 0.25$ mM, $C_{DPH} = 1$ μM.

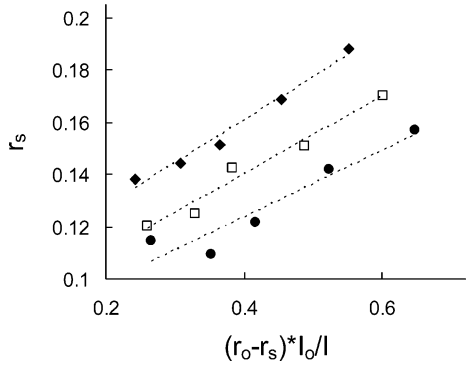

Figure 2. The effect of the $C_{16}Py^+$ concentration on the anisotropy of the DPH fluorescence in the BIC at 25 (solid diamonds), 30 (open squares), and 35 °C (solid circles). The dashed lines represent the least-squares fit of the data ($R^2 = 0.98$, 0.97, and 0.90, correspondingly). $r_o = 0.38$ is the zero anisotropy value of DPH fluorescence; r_s is the steady-state anisotropy (see text for details). $C_{PMA} = C_{HTAB} = 0.25$ mM, $C_{DPH} = 1$ μM.

TABLE 1: Fluorescence Anisotropy Parameters for the Surfactant Micelles and the BIC[a]

	ϕ_{rel}			
T, °C	HTAB	BIC	BIC + butanol	BIC + dodecanol
25		0.17		0.45
30	0.1	0.15	0.17	0.35
35	0.09	0.15	0.21	0.29
40	0.09			
		$S = (r_\infty/r_o)^{1/2}$		
25		0.49		0.33
30	0.33	0.46	0.36	0.33
35	0.33	0.40	0.28	0.33
40	0.33			

[a] Rotational relaxation time ϕ_{rel} is obtained as the relative value normalized by the lifetime τ_o at each temperature. The later decreases, as the temperature increases, which should be taken into account when comparing ϕ_{rel} values at different temperatures. Order parameter *S* values are obtained as a free parameter and should be comparable as long as the assumptions, outlined in the Appendix, hold equally well at different temperatures.

(99%), and 1-dodecanol (98%) were purchased from Aldrich Co. and used as received. All of the solutions were prepared with deionized water (18 MOm), purified by Water Pro PS 90007-00 (Labconco Co.)

Methods. BIC dispersions were prepared, as described in our previous reports, by mixing block ionomer and surfactant in aqueous solutions.[15] Effective hydrodynamic diameter D_{eff} and ζ potential of the BIC dispersion particles were determined by dynamic light scattering, using a Zeta Plus Analyzer with the Multi Angle Sizing option (Brookhaven Co.) and the manufacturer provided software. Alcohols (except dodecanol) were directly added as aqueous solutions. Dodecanol was presolubilized in the HTAB micelles by repeated heating and cooling of the dispersion, until the mixture was completely clear.

To incorporate the DPH probe into HTAB micelles, a methanol solution of DPH was first evaporated in a vial, then a micellar solution of HTAB (10 mM) was added and the probe was solubilized with gentle agitation. Solutions were allowed to equilibrate for at least 24 h (no differences in DPH incorporation were observed for longer equilibration times). These solutions were subsequently used for preparing the BIC. This method proved to yield lower intersample variation than solubilization of the DPH film by preformulated BIC dispersions. No significant changes in BIC particle size and dispersion stability were observed, as compared to DPH-free BIC.

Fluorescence measurements were performed with a RF5000U spectrofluorometer (Simadzu Co.) equipped with manual polarizers, and a Cary Eclipse spectrofluorophotometer (Varian Co.) equipped with automatic polarizers. The temperature was controlled by a water bath within ±0.5 °C. *G*-factors were measured individually for each sample at each temperature. Anisotropy values were always corrected for turbidity-dependent depolarization,[34,35] although, in most cases, these corrections amounted to less than 2% of the total anisotropy values. Only for the BIC containing more than 50% of dodecanol (with respect to HTAB) did the corrections amount to 10% of the total anisotropy. The turbidity was measured with a Shimadzu UV-160 spectrophotometer.

Results and Discussion

Fluorescence Anisotropy in BIC and HTAB Micelles. Figure 1 presents the modified versions of the Stern−Volmer plot for the $C_{16}PyBr$ quenching of the DPH fluorescence in the BIC dispersion at three different temperatures (30, 35, and 40 °C). The data are presented as $1/I$ (rather than I_o/I plot) to separate the curves, which would otherwise overlap. $C_{16}PyBr$ was chosen as a quencher, because it is structurally similar to HTAB. To avoid significant alterations of the BIC structure the ratio of $C_{16}PyBr$ to HTAB was less than 5% in all experiments. The plots were almost perfectly linear in the range of quencher concentrations studied, and the quenching efficiencies increased as the temperature increased, indicating that the quenching was dynamic (see the Appendix for a brief account of the fluorescence anisotropy and quenching in ordered environments). This allowed us to calculate the relative fluorescence lifetimes of the probe, τ/τ_o (τ_o is the lifetime in the absence of the quencher), directly from the fluorescence intensity measurements as $\tau_o/\tau = I_o/I$ (see the Appendix).

Figure 2 presents the plots of the steady-state anisotropy of DPH, r_s, in BIC dispersion vs $(r_o - r_s)\tau_o/\tau$. At every temperature, the data were well fitted by the linear functions, in accordance with eq III presented in the Appendix. This indicated that the simplest model (single fluorescence lifetime, single rotational relaxation time) described the behavior of DPH in BIC reasonably well. The slope values, corresponding to the relative rotational relaxation time, ϕ/τ_o, and the order parameter values, *S*, are presented in Table 1.

QRFA experiments were performed with HTAB micelles to determine the DPH fluorescence anisotropy parameters in the

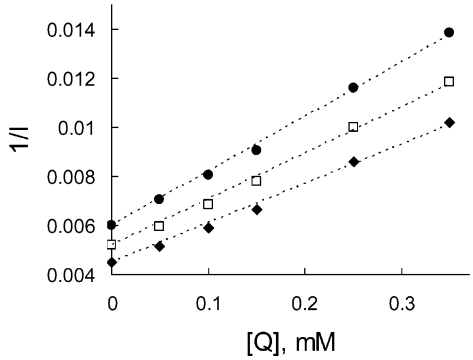

Figure 3. The effect of the $C_{16}Py^+$ concentration on the intensity of the DPH fluorescence in the HTAB micelles at 30 (solid diamonds), 35 (open squares), and 40 °C (solid circles). The dashed lines represent the least-squares fit of reciprocal intensity values ($R^2 > 0.99$ in each case). Fluorescence intensity at zero concentration of the quencher was included as a variable parameter and "unquenched" intensity I_o recovered from the intercept of the fitting line with the *Y*-axis. [Q] is the concentration of the quencher; au = arbitrary fluorescence units. $C_{HTAB} = 5$ mM, $C_{DPH} = 5$ μM.

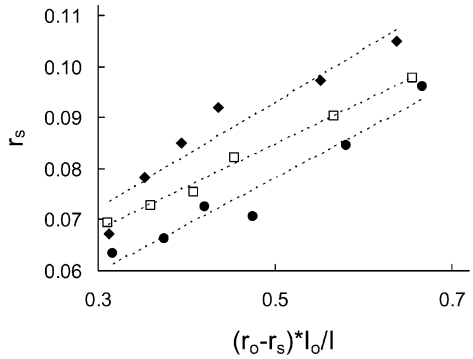

Figure 4. The effect of the $C_{16}Py^+$ concentration on the anisotropy of the DPH fluorescence in the HTAB micelles at 30 (solid diamonds), 35 (open squares), and 40 °C (solid circles). The dashed lines represent the least-squares fit of the data ($R^2 = 0.93$, 0.99, and 0.93, correspondingly). $r_o = 0.38$ is the zero anisotropy value of DPH fluorescence;[28] r_s is the steady-state anisotropy (see text for details). $C_{HTAB} = 5$ mM, $C_{DPH} = 5$ μM.

absence of the block ionomer. Figure 3 presents the Stern−Volmer plots for $C_{16}PyBr$ quenching of the micelle-solubilized DPH. As in the case of the BIC, these plots were linear and the quenching constant increased as the temperature increased, indicating that the quenching was dynamic and that the relative fluorescence lifetimes can be directly estimated. Figure 4 presents the steady-state anisotropy data for the micelle-solubilized DPH at various quenching degrees. The corresponding ϕ/τ_o and *S* values are also presented in Table 1.

The relative rotational relaxation times for BIC were considerably higher than those for HTAB micelles at every temperature studied. This effect reflected (i) slower rotation of the DPH probe due to the higher microviscosity in the BIC and/or (ii) slower rotation of the BIC particles as a whole. Since the diameter of BIC particles was ca. 80 nm[33b] their rotation on the relevant time scale can be neglected. Furthermore, the rate of the micelle rotation $(\phi_{mic}/\tau_o)^{-1}$ was calculated and used to estimate a corrected relaxation time, ϕ_{corr}/τ_o, for the "immobilized" HTAB micelles. (ϕ_{corr}/τ_o was estimated as $1/[(\phi_{exp}/\tau_o)^{-1} - (\phi_{mic}/\tau_o)^{-1}]$, where ϕ_{exp}/τ_o is the experimetnal value for the DPH in the HTAB micelle and ϕ_{mic}/τ_o was calculated as described elsewhere,[36,37] using the published values of DPH fluorescence lifetime, $\tau_o = 8$ ns.[30]) This corrected relaxation time ϕ_{corr}/τ_o did not exceed 0.105, which was still significantly less than the 0.15 measured for BIC. Thus, we concluded that difference in the relaxation times observed between the micelles and BIC was to a significant extent due to the increase in the microviscosity of the surfactant hydrocarbon group region. Notably, the relaxation times for the micelles and BIC slightly decreased as the temperature increased, which was consistent with the expected temperature dependence of the microviscosity.

The order parameters for the BIC were also significantly higher than those for the micelles (Table 1). This could indicate that the HTAB aliphatic groups were more ordered in the BIC than in the micelles. However, it is important to note that the order parameter was also affected by the rotation of the particle as a whole. If one assumed that the rotation of the HTAB micelles was completely stopped upon their incorporation in BIC, the resulting *S* values would be comparable to those observed in the experiment. (S_{corr} was estimated as $S_{exp}(1 + \tau_o/\phi_{mic})^{1/2}$, where S_{exp} is the experimental value for the DPH in the HTAB micelle and τ_o/ϕ_{mic} was calculated as described above.) Thus, based on the steady-state experiments only it was difficult to distinguish between the two limiting cases: (1) incorporation in BIC hinders the rotation of individual micelles without affecting the order of the surfactant alkyl groups within the micelle or (2) incorporation in BIC does not significantly affect the rotation of individual micelles, but increases the order of the surfactant alkyl groups. Overall, the order parameters for DPH in the BIC were significantly smaller than those for DPH in biological and synthetic membranes at similar temperatures ($S = 0.6-0.9$).[24,38] This indicates a relatively low degree of ordering within the surfactant alkyl group domains of the BIC.

Effect of Alcohols on BIC. Figure 5a demonstrates the changes of the steady-state fluorescence anisotropy of DPH, r_s, upon addition of various aliphatic alcohols to BIC. The magnitude and direction of the changes depended on the length of the alcohol chain: the r_s decreased as the short-chain butanol was added and increased as the long-chain dodecanol was added. The effects of the medium-chain hexanol and octanol were bimodal: the alcohols increased the r_s at low concentrations and decreased it at high concentrations. The effective concentrations of alcohols differed by several orders of magnitude, which obviously reflected differences in their partitioning into the hydrophobic regions of the BIC. Figure 5b presents the same anisotropy data as the dependencies of r_s vs the alcohol-to-surfactant ratio C_{inc}/C_{HTAB}, where C_{inc} is the concentration of the alcohol incorporated in the BIC and C_{HTAB} is the concentration of HTAB. C_{inc} values were estimated by using the known octanol−water partitioning coefficients.[39] As is seen in the figure, the most notable increases of the r_s were observed as the alcohol-to-surfactant ratios reached ca. 0.2, independent of the nature of alcohol. The only alcohol that did not increase the r_s at any concentration was butanol. As the C_{inc}/C_{HTAB} ratio increased, the r_s greatly decreased for butanol, somewhat decreased for hexanol and octanol, and did not change for dodecanol.

The effects of alcohols were further characterized by using the QRFA method. Two systems were chosen for these experiments: one displaying a large decrease in the r_s (0.1 M butanol) and another displaying a large increase in the r_s (0.05 mM dodecanol). The calculated alcohol-to-surfactant ratios, C_{inc}/C_{HTAB} for both systems, were approximately the same (ca. 0.25). The results of the QRFA experiments are presented in Figure 6. These data were relatively well fitted by the linear functions. The values of ϕ/τ_o and *S* are presented in Table 1. This study suggested that both butanol and dodecanol decreased the order parameters significantly. It is noteworthy that the size of the BIC complexes was not drastically altered by the alcohols as

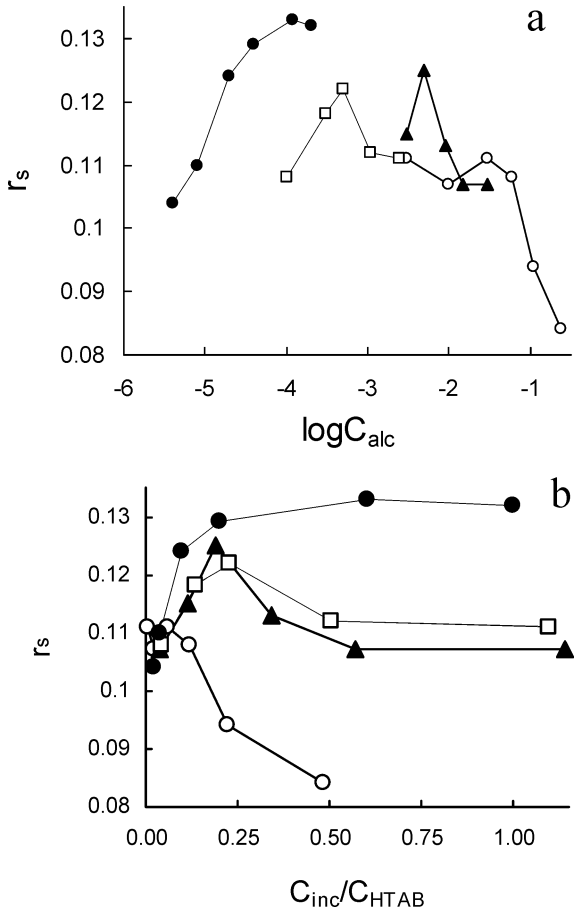

Figure 5. The effects of 1-butanol (open circles), 1-hexanol (solid triangles), 1-octanol (open squares), and 1-dodecanol (solid circles) concentration on the anisotropy of the DPH fluorescence in the BIC at 30 °C. (a) C_{alk} is the total concentration of the alcohol in the mixture. (b) C_{inc}/C_{HTAB} is the calculated molar ratio of alcohol to surfactant in the BIC. The amount of the incorporated alcohol was calculated assuming that it simply partitions between the aqueous phase of volume V_{aq} and the hydrophobic BIC phase of volume V_h (see text for details). $C_{PMA} = C_{HTAB} = 0.25$ mM, $C_{DPH} = 1$ μM.

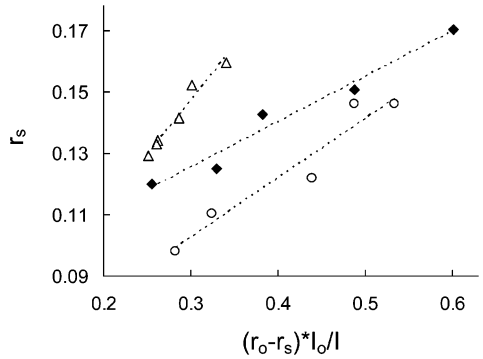

Figure 6. The effect of the $C_{16}Py^+$ concentration on the anisotropy of the DPH fluorescence at 30 °C in the BIC in the absence of alcohols (solid diamonds) and in the presence of 1-butanol (0.1 M, open circles) or 1-dodecanol (0.05 mM, open triangles). The dashed lines represent the least-squares fit of the data ($R^2 = 0.97$, 0.93, and 0.96, correspondingly). $r_o = 0.38$ is the zero anisotropy value of DPH fluorescence;[28] r_s is the steady-state anisotropy (see text for details). $C_{PMA} = C_{HTAB} = 0.25$ mM, $C_{DPH} = 1$ μM.

determined by dynamic light scattering (data not shown). Thus, the changes in the *S* values most likely reflect decreases of the surfactant hydrocarbon group ordering within the BIC. Since the hydroxyl groups of the alcohols are supposedly "locked" in the headgroup regions of the surfactants and the hydrocarbon

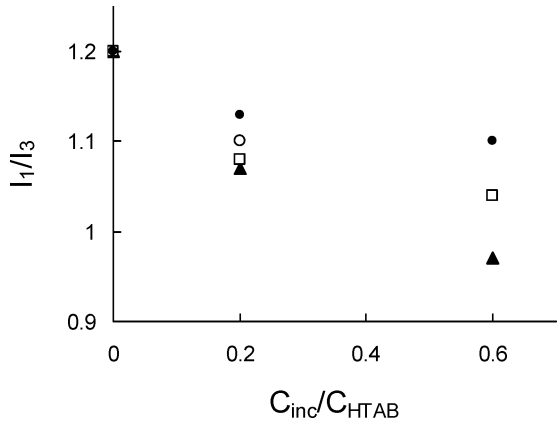

Figure 7. The effects of 1-butanol (open circles), 1-hexanol (solid triangles), 1-octanol (open squares), and 1-dodecanol (solid circles) concentration on the I_1/I_3 ratio of the fluorescence spectra of pyrene in the BIC at 30 °C. C_{inc}/C_{HTAB} is the calculated molar ratio of alcohol to surfactant in the BIC. $C_{PMA} = C_{HTAB} = 0.25$ mM, $C_{DPH} = 1$ μM.

chains of the alcohols are shorter than those of the surfactants, the incorporation of the alcohols should create "gaps" in the surfactant hydrocarbon group regions. Indeed, the surfactant alkyl groups are known to acquire less extended conformations in the mixed surfactant−alcohol aggregates than in the alcohol-free aggregates.[40] Conversely, alcohols have more extended conformations in the mixed aggregates than in the free state.[40,41] Thus, the decreases in the surfactant hydrocarbon group order can result from the need to compensate the mismatch in the lengths of the hydrocarbon groups of the alcohol and surfactant.

The decrease of the DPH order parameters in BIC, caused by the addition of alcohols, was accompanied by the increase in the rotational relaxation times (Table 1). It is possible that incorporation of small uncharged hydroxyl groups of the alcohols between the surfactant headgroups reduced the lateral repulsion of the molecules and increased their net attraction, which resulted in higher microviscosity. Furthermore, it has been suggested, based on the changes in micropolarity, that addition of alcohols leads to expulsion of the water molecules from the micelle core and headgroups regions.[42,43] As shown in Figure 7, addition of the alcohols to the BIC leads to the decrease of the intensity ratio of the first and third peaks in the fluorescence spectra of pyrene (I_1/I_3). This indicates that the polarity in the aliphatic groups region is decreasing, probably due to water expulsion. Substitution of the smaller water molecules by the larger alcohol molecules might also contribute to the increase of the microviscosity. The increases in the relaxation times were very pronounced in the case of dodecanol and less pronounced for butanol. This may explain different effects of these alcohols on the fluorescence anisotropy. Indeed, the decrease of the order parameter is consistent with the decrease in r_s induced by butanol. Conversely, a severalfold increase in the relaxation time with dodecanol may offset the decrease of the order parameter and result in the overall increase of the fluorescence anisotropy.

Overall, addition of alcohols is known to produce multiple changes in surfactant[44−48] and polymer−surfactant aggregates.[49−52] In terms of packing parameters (*P*),[53] aliphatic alcohols have *P* larger than 1, indicating their preference for inversed micelle morphologies. Upon mixing with single tail ionic surfactants, such as HTAB, which have *P* in the order of $^1/_3$−$^1/_2$ and prefer spherical or cylindrical micelle morphology, the alcohols increase the average packing parameter. Therefore, addition of aliphatic alcohols leads to the transition of the aggregates from spherical to cylindrical, lamellar, and eventually reversed micelle morphology.[54] Such a transition should obviously be connected

with the changes in the surfactant alkyl groups packing, especially in the cases when the lengths of the surfactant and alcohol groups differ significantly. These changes have been widely described for liposome and biological membranes as exhibited by variations of phase transition temperatures and microviscosity.[55−57] This study suggests that the addition of alcohols alters surfactant packing and dynamics within the BIC as well. Studying these effects in relation to the properties of the alcohols (in particular, their chain length) is important for better understanding self-assembly in BIC, as well as for discovering ways to alter the BIC properties for practical applications.

Conclusions

This study provides ample evidence, based on the measurements of the DPH fluorescence anisotropy, that the structure of the surfactant domains in the BIC and micelles is quite different. Specifically, the rotational relaxation of DPH probe in BIC was considerably slower than that in the micelles. This suggested that the hydrocarbon regions formed by the surfactant alkyl groups in BIC displayed higher microviscosity due to the binding of the surfactant headgroups to the polyion chain. The order parameter was also higher in the BIC compared to the micelles. This was indicative of a greater extent of alignment of the surfactant alkyl groups in the BIC. It could also reflect slower rotational movement of the BIC particles as a whole compared to the micelles. Despite some increase in the order parameter it was unlikely that the surfactant alkyl groups in the BIC were highly ordered (e.g. crystalline or liquid crystalline) as the order parameter was still well below that of the lipid gel phase. Furthermore, the order parameters, as well as the rotational relaxation times, were strongly affected by addition of aliphatic alcohols of various chain lengths. Decrease of the order parameter, caused by the addition of the alcohols, was attributed to the changes in the conformation of the alkyl groups of the surfactant that may be needed to "fill the gaps" induced by the shorter alcohol alkyl groups. The increase of the rotational relaxation time, especially pronounced in the case of dodecanol, was attributed to the decreased repulsion of the surfactant headgroups in the mixed aggregates as well as to the expulsion of water from the BIC interior evidenced by the decrease in the micropolarity. Overall, addition of the aliphatic alcohols provides a route to modify the nonpolar regions of the BIC, which can be useful in drug delivery and other applications of these systems.

Appendix. Fluorescence Anisotropy in Ordered Environments

Rotational motion of the probe decreases the fluorescence anisotropy. For a simple rotator (rodlike molecules, such as DPH) in an isotropic solution the steady-state value of the fluorescence anisotropy, r_s, is expressed as follows:

$$r_s = r_o/(1 + \tau/\phi) \qquad \text{(I)}$$

where r_o is the intrinsic anisotropy, τ is the fluorescence lifetime, and ϕ_i is the rotational relaxation time, dependent on the local viscosity, i.e., *microviscosity*. (Multiple relaxation times ϕ_i are often needed to adequately describe the anisopy decay.[28] For simplicity, eq I uses a single relaxation time as an *effective* relaxation time. Limitations of this approach are briefly discussed by Hare.[59]) Thus the relative microviscosities of different solutions can be assessed by comparing the r_s values.

The situation is more complex for the probe incorporated into an organized environment (e.g., a surfactant aggregate), which itself is anisotropic. Anisotropy of the media restricts rotations of the probe and certain orientations are essentially prohibited. Thus, the residual fluorescence anisotropy term, r_∞ (also called "limiting anisotropy"), is usually introduced as follows:

$$r_s = r_\infty + (r_o - r_\infty)/(1 + \tau/\phi) \qquad \text{(II)}$$

For a rodlike molecule such as DPH, which has excitation and emission dipoles parallel to the long molecular axis, the limiting anisotropy can be converted into the order parameter, S: $S^2 = r_\infty/r_o$.[26,27] This parameter reflects the degree of alignment of the probe molecules: $S = 0$ suggests no alignment and $S = 1$ suggests complete alignment. In an anisotropic environment the order parameter of the probe is closely related to the order parameter of the environment.[28]

The relaxation times and the degrees of order can be determined from the steady-state measurements by using the QRFA method suggested by Lakowicz et al.[24] In this method the fluorescence lifetime is altered by adding various concentrations of the dynamic quencher and the changes of the steady-state anisotropy r_s are measured. Assuming that the r_∞ and ϕ values are not affected (which is generally correct at low concentrations of the quencher), the quenching can be analyzed by using a linear regression r_s vs $(r_o - r_s)\tau_o/\tau$:

$$r_s = r_\infty + \phi/\tau_o[(r_o - r_s)\tau_o/\tau] \qquad \text{(III)}$$

where τ_o and τ are the lifetimes in the absence and presence of the quencher. This yields the normalized value ϕ/τ_o as the slope and r_∞ as the intercept.

The effect of the quencher on the fluorescence lifetime is expressed as follows:

$$\tau_o/\tau = 1 + K_D[Q] \qquad \text{(IV)}$$

where K_D is the dynamic quenching constant and [Q] is the concentration of the quencher.

The value of K_D can be determined from the Stern−Volmer plots. Generally, the contributions of the dynamic and static quenching should be considered:[25]

$$I_o/I = (1 + K_D[Q])(1 + K_S[Q]) \qquad \text{(V)}$$

where I_o and I are the initial and quenched fluorescence intensity, respectively, and K_S is the static quenching constant. The combination of the two quenching mechanisms results in the upward curvature of the Stern−Volmer plot. The analysis is simplified if the plot is linear suggesting that one mechanism has a negligible contribution. In this case the dynamic and static mechanisms are discriminated by comparing the plots obtained at different temperatures.[25] If the static quenching can be neglected τ_o/τ equals I_o/I. For further extensive consideration of the theoretical and practical aspects of fluorescence anisotropy see, for example, Lakowicz[25] and references therein.

Acknowledgment. The authors acknowledge the financial support of this work by the NSF, U.S.A. (DMR-0071682), and NSERC, Canada (STR-0181003), and J. A. Vetro for reading the manuscript.

References and Notes

(1) *Interaction of Surfactants with Polymers and Proteins*; Goddard, E. D., Ananthapadmanabhan, K. P., Eds.; CRC Press: Boca Raton, FL, 1993.

(2) Hansson, P. *Langmuir* **2001**, *17*, 4167.
(3) Hansson, P.; Almgren, M. *J. Phys. Chem.* **1995**, *99*, 16684.
(4) Hansson, P.; Almgren, M. *J. Phys. Chem.* **1995**, *99*, 16694.
(5) Groot, R. D. *Langmuir* **2000**, *16*, 7493.
(6) Hansson, P.; Almgren, M. *Langmuir* **1994**, *10*, 2115.
(7) (a) Kasaikin, V. A.; Wasserman, A. M.; Zakharova, J. A.; Motyakin, M. V.; Kolbanovsky, A. D. *Colloids Surf. A* **1999**, *147*, 169. (b) Wasserman, A. M.; Kasaikin, V. A.; Zakharova, Yu. A.; Aliev, I. I.; Baranovsky, V. Yu.; Doseva, V.; Yashina, L. L. *Spectrochim. Acta, Part A* **2002**, *58*, 1241.
(8) Lindman, B.; Thalberg, K. In *Interaction of Surfactants with Polymers and Proteins*; Goddard, E. D., Ananthapadmanabhan, K. P., Eds.; CRC Press: Boca Raton, FL, 1993; Chapter 5.
(9) Kabanov, V. A.; Zezin, A. B.; Rogacheva, V. B.; Khandurina, Y. V.; Novoskoltseva, O. A. *Macromol. Symp.* **1997**, *126*, 79.
(10) Antonietti, M.; Conrad, J. *Angew. Chem., Int. Ed. Engl.* **1994**, *33*, 1869.
(11) Antonietti, M.; Conrad, J.; Thunemann, A. *Macromolecules* **1994**, *27*, 6007.
(12) Antonietti, M.; Maskos, M. *Macromol. Rapid Commun.* **1995**, *16*, 763.
(13) Chu, B.; Yeh, F.; Sokolov, E. L.; Starobudtsev, S. G.; Khokhlov, A. R. *Macromolecules* **1995**, *28*, 8447.
(14) Zhou, S.; Yeh, F.; Burger, C.; Chu, B. *J. Phys. Chem. B* **1999**, *103*, 2107.
(15) Bronich, T. K.; Kabanov, A. V.; Kabanov, V. A.; Yu, K.; Eisenberg, A. *Macromolecules* **1997**, *30*, 3519.
(16) Kabanov, A. V.; Bronich, T. K.; Kabanov, V. A.; Yu, K.; Eisenberg, A. *J. Am. Chem. Soc.* **1998**, *120*, 9941.
(17) Thünemann, A. F.; Beyermann, J.; Kukula, H. *Macromolecules* **2000**, *33*, 5906.
(18) Herve, P.; Destarac, M.; Berret, J.-F.; Lal, J.; Oberdisse, J.; Grillo, I. *Europhys. Lett.* **2002**, *5*, 912.
(19) Bronich, T. K.; Popov, A. M.; Eisenberg, A.; Kabanov, V. A.; Kabanov, A. V. *Langmuir* **2000**, *16*, 481.
(20) Bronich, T. K.; Ouyang, M.; Eisenberg, A.; Kabanov, V. A.; Szoka, F. C., Jr.; Kabanov, A. V. *Polym. Prepr.* **2000**, *41*, 1645.
(21) Solomatin, S. V.; Bronich, T. K.; Eisenberg, A.; Kabanov, V. A.; Kabanov, A. V. *Langmuir* **2004**, *20*, 2066.
(22) Li, Y.; Xu, R.; Couderc, S.; Bloor, D. M.; Warr, J.; Penfold, J.; Holzwarth, J. F.; Wyn-Jones, E. *Langmuir* **2001**, *17*, 5657.
(23) Berret, J.-F.; Herve, P.; Aguerre-Chariol, O.; Oberdisse, J. *J. Phys. Chem. B* **2003**, *107*, 8111.
(24) Lakowicz, J. R.; Prendergast, F. G.; Hogen, D. *Biochemistry* **1979**, *18*, 520.
(25) Lakowicz, J. R. *Principles of Fluorescence Spectroscopy*; Plenum Press: New York, 1983.
(26) Kinosita, K.; Kawato, S.; Ikegami, A. *Biophys. J.* **1977**, *20*, 289.
(27) Lipari, G.; Szabo, A. *Biophys. J.* **1980**, *30*, 489.
(28) Jahnig, F. *Proc. Natl. Acad. Sci. U.S.A.* **1979**, *76*, 6361.
(29) Ameloot, M.; Hendrix, H.; Herreman, W.; Pottel, H.; van Cauwelart, F.; van der Meer, W. *Biophys. J.* **1984**, *46*, 525.
(30) van der Meer, B. W.; van Hoeven, R. P.; van Blitterswijk, W. J. *Biochim. Biophys. Acta* **1986**, *854*, 38.
(31) Shinitzky, M.; Dianoux, A.-C.; Gitler, C.; Weber, G. *Biochemistry* **1971**, *10*, 2106.
(32) Shinitzky, M. *Isr. J. Chem.* **1974**, *12*, 879.
(33) (a) Wang, J.; Varshney, S. K.; Jerome, R.; Teyssie, P. *J. Polym. Sci., Part A: Polym. Chem.* **1992**, *30*, 2251. (b) Solomatin, S. V.; Bronich, T. K.; Eisenberg, A.; Kabanov, V. A.; Kabanov, A. V. *Langmuir* **2003**, *19*, 8069.
(34) Teale, F. W. *Photochem. Photobiol.* **1969**, *10*, 363.
(35) Lentz, B. R.; Moore, B. M.; Barrow, D. A. *Biophys. J.* **1979**, *25*, 489.
(36) Quitevis, E. L.; Marcus, A. H.; Fayer, M. D. *J. Phys. Chem.* **1993**, *97*, 5762.
(37) Berr, S.; Jones, R. R. M.; Johnson, J. M., Jr. *J. Phys. Chem.* **1992**, *96*, 5611.
(38) van Blitterswijk, W. J.; van Hoeven, R. P.; van der Meer, B. W. *Biochim. Biophys. Acta* **1981**, *644*, 323.
(39) Kamlet, M. J.; Doherty, R. M.; Abraham, M. H.; Marcus, Y.; Taft, R. F. *J. Phys. Chem.* **1988**, *92*, 5244.
(40) Sasanuma, Y.; Nishimura, F.; Wakabayashi, H.; Suzuki, A. *Langmuir* **2004**, *20*, 665.
(41) Suzuki, A.; Miura, N.; Sasanuma, Y. *Langmuir* **2000**, *16*, 6317.
(42) Neumann, M. G.; de Sena, G. L. *Colloid Polym Sci.* **1997**, *275*, 648.
(43) Muto, Y.; Yoda, K.; Yoshida, N.; Esumi, K.; Meguro, K.; Zana, R.; Binana-Limbele, W. *J. Colloid Interface Sci.* **1989**, *130*, 165.
(44) Ekwall, P.; Mandell, L. *Acta Chem. Scand.* **1967**, *21*, 1612.
(45) Stilbs, P. *J. Colloid Interface Sci.*, **1982**, *89*, 547.
(46) Leung, R.; Shah, D. O. *J. Colloid Interface Sci.* **1986**, *113*, 484.
(47) Zana, R. *Adv. Colloid Interface Sci.* **1995**, *57*, 1.
(48) Førland, G. M.; Samseth, J.; Gjerde, M.; Høiland, H.; Jensen, A. Ø.; Mortensen, K. *J. Colloid Interface Sci.* **1998**, *203*, 328.
(49) Fukui, H.; Satake, I.; Hayakawa, K. *Langmuir* **2002**, *18*, 4465.
(50) Shirahama, K.; Koga, H.; Takisawa, N. *Prog. Colloid Polym. Sci.* **2003**, *122*, 82.
(51) Khandurina, Yu. V.; Rogacheva, V. B.; Zezin, A. B.; Kabanov, V. A. *Vysokomol. Soedin., Ser. A Ser. B* **1994**, *36*, 241.
(52) Makhaeva, E. E.; Starodubtzev, S. G. *Makromol. Chem., Rapid Commun.* **1993**, *14*, 105.
(53) Israelachvili, J. N.; Mitchell, D. J.; Ninham, B. W. *Biochim. Biophys. Acta* **1977**, *470*, 185.
(54) Jönsson, B.; Wennerstrom, H. *J. Phys. Chem.* **1987**, *91*, 338.
(55) Kamaya, H.; Matubayasi, N.; Ueda, I. *J. Phys. Chem.* **1984**, *88*, 797.
(56) Kitagawa, S.; Hirata, H. *Biochim. Biophys. Acta* **1992**, *1112*, 14.
(57) Firestone, L. L.; Alimoff, J. K.; Miller, K. W. *Mol. Pharm.* **1994**, *46*, 508.
(58) McIntosh, T. J.; Lin, H.; Li, S.; Huang, C. *Biochim. Biophys. Acta* **2001**, *1510*, 219.
(59) Hare, F. *Biophys. J.* **1983**, *42*, 205.